Molecular Cell, Vol. 17, 773–782, March 18, 2005, Copyright ©2005 by Elsevier Inc. DOI 10.1016/j.molcel.2005.02.023

Defining a Centromere-like Element in *Bacillus subtilis* by Identifying the Binding Sites for the Chromosome-Anchoring Protein RacA

Sigal Ben-Yehuda,[1,2,7] Masya Fujita,[1,7] Xiaole Shirley Liu,[3] Boris Gorbatyuk,[1] Dunja Skoko,[4] Jie Yan,[4] John F. Marko,[4] Jun S. Liu,[5] Patrick Eichenberger,[1,8] David Z. Rudner,[1,6] and Richard Losick[1,*]

[1]Department of Molecular and Cellular Biology
Harvard University
16 Divinity Avenue
Cambridge, Massachusetts 02138
[2]Department of Molecular Biology
Faculty of Medicine
The Hebrew University of Jerusalem
911120 Jerusalem
Israel
[3]Department of Biostatistics and Computational Biology
Dana-Farber Cancer Institute
Harvard School of Public Health
Boston, Massachusetts 02115
[4]Department of Physics
University of Illinois at Chicago
845 West Taylor Street
Chicago, Illinois 60607
[5]Department of Statistics
Harvard University
1 Oxford Street
Cambridge, Massachusetts 02138
[6]Department of Microbiology and Molecular Genetics
Harvard Medical School
200 Longwood Avenue
Boston, Massachusetts 02115

Summary

Chromosome segregation during sporulation in *Bacillus subtilis* involves the anchoring of sister chromosomes to opposite ends of the cell. Anchoring is mediated by RacA, which acts as a bridge between a centromere-like element in the vicinity of the origin of replication and the cell pole. To define this element we mapped RacA binding sites by performing chromatin immunoprecipitation in conjunction with gene microarray analysis. RacA preferentially bound to 25 regions spread over 612 kb across the origin portion of the chromosome. Computational and biochemical analysis identified a GC-rich, inverted 14 bp repeat as the recognition sequence. Experiments with single molecules of DNA demonstrated that RacA can condense nonspecific DNA dramatically against appreciable forces to form a highly stable protein-DNA complex. We propose that interactions between DNA bound RacA molecules cause the centromere-like element to fold up into a higher order complex that fastens the chromosome to the cell pole.

*Correspondence: losick@mcb.harvard.edu
[7]These authors contributed equally to this work.
[8]Present address: Department of Biology, New York University, 100 Washington Square East, New York, NY 10003.

Introduction

Dividing cells face the challenge of segregating newly duplicated chromosomes with high fidelity to ensure that progeny are genetically identical. This challenge is particularly acute in cells that divide asymmetrically, which must faithfully segregate sister chromosomes to progeny that are often decidedly unequal in size. Asymmetric cell division occurs in eukaryotes and prokaryotes as a basic mechanism for generating cellular diversity (Horvitz and Herskowitz, 1992; Gonczy and Hyman, 1996). For example, asymmetric division of zygotes decides cell fates at the early stages of development in the soil nematode *Caenorhabditis elegans* and in the flowering plant *Arabidopsis thaliana* (Gonczy and Hyman, 1996; Scheres and Benfey, 1999). Likewise, asymmetric division by the budding yeast *Saccharomyces cerevisiae* and the dimorphic bacterium *Caulobacter crescentus* helps maintain polarity and dictates the dissimilar fates of the products of cytokinesis (Madden and Snyder, 1998; Jensen et al., 2002; Ausmees and Jacobs-Wagner, 2003; Nelson, 2003).

Here, we are concerned with chromosome segregation during asymmetric division by *Bacillus subtilis*. This spore-forming bacterium, which has a single, circular chromosome, exhibits alternative modes of cell division. Under conditions of growth it divides by binary fission, segregating sister chromosomes to equal-sized progeny. During sporulation, however, the bacterium divides asymmetrically, forming a septum near a pole of the developing cell (sporangium). Formation of this polar septum divides the sporangium into two compartments called the forespore and the approximately eight-times larger mother cell (Stragier and Losick, 1996; Piggot and Losick, 2001). By what mechanisms does the sporangium ensure that the forespore and the mother cell each receive a chromosome and how does it do so with high efficiency? Chromosome segregation during sporulation takes place in three stages. First, the sister chromosomes are remodeled into a single elongated, serpentine-like DNA mass (nucleoid) called the axial filament (Ryter et al., 1966). The axial filament extends from pole to pole, with the replication origin region of each chromosome anchored at extreme opposite ends of the sporangium (Glaser et al., 1997; Lin et al., 1997; Webb et al., 1997). Next, the polar septum forms and traps the origin-proximal portion of one chromosome (representing about one-third of the genome) in the newly formed forespore. The remaining two-thirds of the chromosome extends across the septum and is initially left behind in the mother cell together with the other sister chromosome (Wu and Errington, 1994). Finally, a DNA translocase assembles around the chromosome at the point at which it transverses the septum and pumps the origin-distal two-thirds of the chromosome across the septum and

into the forespore (Wu and Errington, 1997; Ben-Yehuda et al., 2003b).

We identified a developmentally regulated gene, *racA* (for remodeling and anchoring of the chromosome), that is required for the formation of the axial filament and for anchoring the origin regions at the cell poles (Ben-Yehuda et al., 2003a). Sporulating cells harboring a *racA* mutation do not produce an axial filament and frequently fail to trap DNA inside the forespore (Ben-Yehuda et al., 2003a; Wu and Errington, 2003). Cytological experiments show that the product of *racA* (RacA) is concentrated at the extreme poles of the sporangium and also exhibits a general, nonspecific association with the entire axial filament. Polar localization depends on the cell division protein DivIVA, which itself localizes at the poles (Marston et al., 1998; Thomaides et al., 2001). In the absence of DivIVA, RacA is concentrated at the outer edges of the nucleoid, where the origins of replication are located, but is not anchored at the extreme poles (Ben-Yehuda et al., 2003a; Wu and Errington, 2003). These findings suggest that RacA binds to sites clustered in the origin portion of the chromosome, which represents a centromere-like element. In this model, the centromere bound RacA molecules form an adhesive structure that directly or indirectly interacts with DivIVA, thereby causing the chromosomes to adhere at the poles. In partial support for this model, chromatin immunoprecipitation (ChIP) experiments revealed that RacA associates not only nonspecifically with the entire chromosome but also with strong preference to regions located close to the origin of replication (Ben-Yehuda et al., 2003a).

To understand the nature of this centromere-like element, we attempted to map the binding sites for RacA on a genome-wide basis and to identify the DNA sequence motif that RacA (or an unknown protein with which it interacts) recognizes. Here, we show that RacA binds with high selectivity to 25 distinct regions distributed over 612 kb across the origin proximal portion of the chromosome (the portion that is trapped in the forespore by the polar septum). We further show that specific binding is achieved by the direct interaction of RacA with a 14 bp long, inverted repeat DNA sequence herein named *ram* (for *R*acA binding *m*otif). Finally, evidence is presented that RacA molecules are able to condense non-*ram*-containing DNA into an extremely stable DNA-protein complex. Based on these observations we propose that RacA is responsible for collapsing much or all of the centromere-like element into a higher order complex.

Results

Genome-Wide Identification of Chromosomal Regions at Which RacA Binds Preferentially

To identify RacA binding regions comprehensively, we performed chromatin immunoprecipitation in conjunction with gene microarray analysis (ChIP-on-chip) (Ren et al., 2000; Iyer et al., 2001; Laub et al., 2002; Molle et al., 2003). In these ChIP-on-chip experiments, DNA fragments recovered from the immunoprecipitation with anti-RacA antibodies were amplified by polymerase chain reaction (PCR) in the presence of Cy5-dUTP. In parallel, total DNA from the formaldehyde-treated cells that had not been subjected to immunoprecipitation was similarly amplified in the presence of Cy3-dUTP. The differentially labeled DNAs were then combined and hybridized to a microarray that had been imprinted with DNAs corresponding to an almost complete set of the open reading frames (ORFs) in the *B. subtilis* genome (Britton et al., 2002; see Experimental Procedures). Figure 1A shows the calculated enrichment factor of the hybridization signal for each gene on the microarray for a representative experiment. (See the Supplemental Data available with this article online. Table S1 shows the full data set from two independent experiments.) The enrichment factor was the ratio of the hybridization signal from the Cy5-labeled DNA from the immunoprecipitation to that from the Cy3-labeled, total DNA. The results were striking, revealing 25 distinct regions of preferential binding with enrichment factors at the peaks ranging from 9-fold to greater than 27-fold. Importantly, all 25 regions were located in the origin-proximal portion of the chromosome, within the portion that is trapped in the forespore compartment by polar septation (shown in the enlargement of Figure 1B and indicated in red in Table S1). Some of the 25 regions were so close to each other that they are not easily distinguishable in Figure 1B but can be seen as being distinct in Table S1. These 25 regions were spread out over a large stretch of the chromosome, extending from position –412 to position +200 kb and covering a 612 kb segment of DNA. Interestingly, this segment is asymmetric with respect to the origin, with twice as much of the DNA and 21 out of the 25 binding regions being located to the left of the origin (Figure 1B, Table S1). Thus, our analysis revealed that RacA anchors the chromosome to the cell pole through a large, centromere-like element composed of multiple binding sites spread out over, and asymmetrically distributed around, the replication origin.

Using Bioinformatics to Identify the RacA Binding Motif

Preferential binding to 25 regions in the origin-proximal region of the chromosome indicates that RacA or a protein with which it associates recognizes a nucleotide sequence motif that is present in each of these regions. To identify this motif computationally, we used a two-step strategy based on Motif Discovery Scan (MDscan, [Liu et al., 2002] and Motif Regressor [Conlon et al., 2003]). MDscan is designed to identify common motifs of specified motif widths in sequences that have been ranked according to their enrichment factor in ChIP-on-chip experiments. We reasoned that RacA binding sites could be inside or outside of the ORFs used in the construction of the microarray. Also, the sonication step of the ChIP procedure would have generated a spectrum of hybridization probes that would have overlapped with ORFs whether or not the specific binding sequences were within the DNA segments on the microarray. Accordingly, for each DNA that exhibited a significant enrichment factor (greater than five), we included 500 bp of upstream and 500 bp of downstream sequences as well as the sequence of the ORF itself in our analysis (see Supplemental Data). In this way, a to-

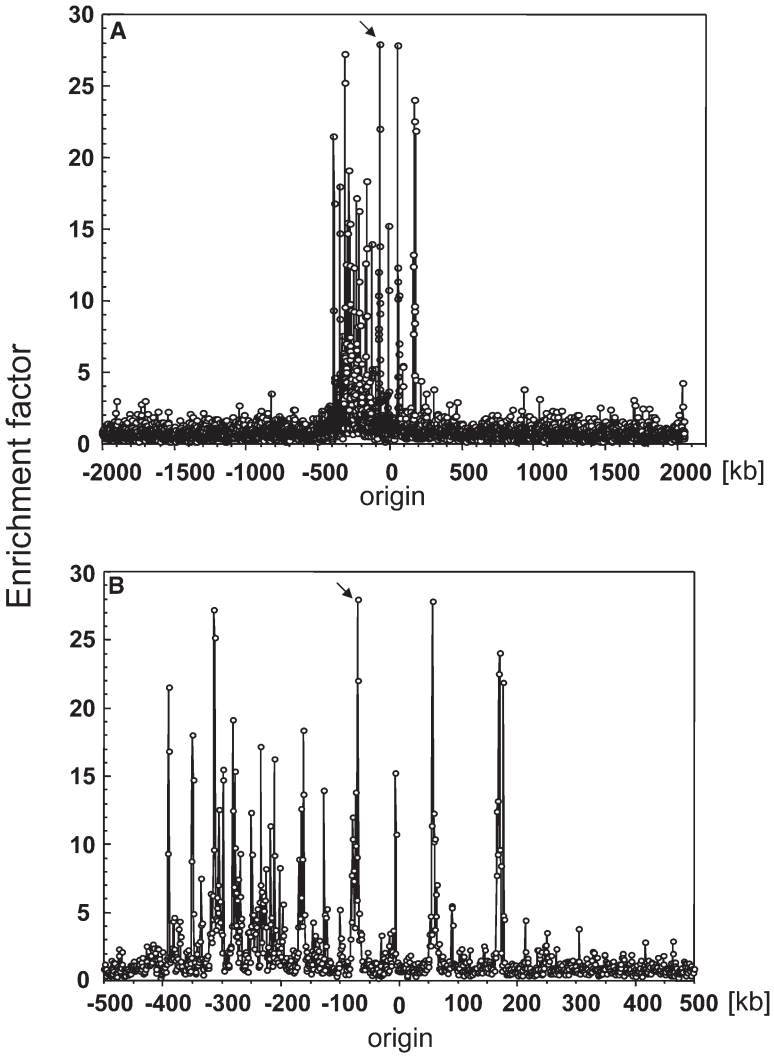

Figure 1. Genome-Wide Mapping of Chromosomal Regions at Which RacA Binds preferentially

(A) Anti-RacA immunoprecipitated DNA and total chromosomal DNA (the DNA prior to the immunoprecipitation) were labeled and hybridized to a microarray chip (ChIP-on-chip analysis) containing almost the entire set of *B. subtilis* ORFs (see the text for details). The enrichment factor for a given ORF was calculated as the ratio of hybridized immunoprecipitated DNA to hybridized total DNA for a representative experiment. Twenty-five distinct binding regions were identified all located at the origin-proximal region. Positions to the left of the origin are identified with a minus symbol and to the right of the origin are identified with no symbol. The full data set is shown in Table S1.

(B) Enlargement of the origin-proximal region (–500 kb – +500 kb) from (A). The arrow indicates a previously identified binding region (Ben-Yehuda et al., 2003a).

tal of 262 candidate motifs were identified by MDscan with widths ranging from 6 to 17 bp. Next, each candidate motif, represented as a position-specific probability matrix, was used to scan each ORF on the array plus flanking sequences and to assign to it a motif-matching score based on the number of sites within the DNA segment that matched the motif (i.e., the number of putative binding sites) and the extent to which each such site matched the motif (i.e., strength of the putative binding site). Then, for each candidate motif, Motif Regressor was used to perform a simple linear regression between the logarithm of the motif matching scores and the logarithm of the enrichment factors observed in the ChIP-on-chip analysis. In principle, a correct motif should exhibit a strong correlation between the motif matching scores and the enrichment factors, whereas incorrect motifs would not. Motif Regressor reports candidate motifs by ascending regression p value, and the best motif reported (Figure 2A) had a p value of <<e-300, an R square of 0.13, and had been ranked the best motif by the MDscan at motif width 14. Linear regression of the motif using only 618 ORFs near the replication origin (200 to the right and 418 to the left) gave an R square of 0.41, which means that considering the presence of this motif alone explains 41% of ChIP-on-chip enrichment variations in the experiment (Figure 2B).

The binding motif predicted by MDscan and Motif Regressor is presented in Figure 2A as a position-specific weight matrix (sequence logo) of 14 bp in length. The logo, which is strikingly rich in GC base pairs, is an inverted repeat, with the most conserved positions at the outer edges. Scanning the peaks of the 25 regions of preferential binding with the sequence logo revealed that all except one (*yxjF*, which had an enrichment factor of 13.5) contained at least one sequence with a significant match to the predicted binding sequence (Table S2). Interestingly, all of the putative binding sites in the peak regions of RacA binding were exclusively located inside ORFs, in contrast to the recognition sequences for transcriptional regulatory proteins, which are generally located in intergenic regions. Also noteworthy was that 20 of the RacA binding regions exhibited multiple copies of the sequence motif clustered

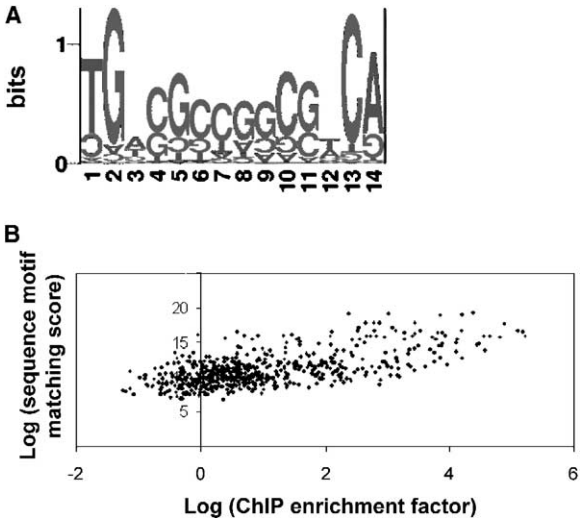

Figure 2. Prediction of a Potential RacA Binding Motif by Use of MDscan and Motif Regressor

(A) Position-specific weight matrix (sequence logo) of the predicted inverted repeat, 14 bp binding motif for RacA as predicted by MDscan and Motif Regressor.

(B) Correlation between ChIP-on-chip enrichment factors and sequence motif matching scores (to the motif in Figure 1) for the 618 ORFs near the replication-origin region in the *B. subtilis* genome. For details see the Supplemental Data.

near each other (that is, either the ORF with the peak enrichment factor or its nearest neighbor contained more than one putative binding site; Table S2). For example, the peak corresponding to adjacent genes *spsC* and *spsD*, which exhibited an enrichment factor of approximately 30, contained four potential binding sequences, two of which had a high motif matching score. Moreover, two additional sites were located within neighboring ORFs, indicating that the peak was generated from as many as six binding sites (five of them being in ORFs with an enrichment factor >9).

The 14 bp Sequence Motif Is Sufficient for RacA Binding In Vivo

As a test of the functional significance of the 14 bp consensus sequence, we performed ChIP experiments in which we translocated a small segment of the chromosome containing the putative recognition sequence for RacA to a site at which preferential binding by RacA is not normally observed. As a donor site we used *ywjI*, a region at which RacA binds with high preference (having an enrichment factor of 20.7, Table S1) and that contained three putative binding sequences, two of which were closely spaced (being separated by 25 bp) and had high motif scores (Table S2). The *ywjI* gene, which is located at position –409.5 kb on the chromosome, encodes a protein of unknown function and is not essential for growth or sporulation (data not shown), making it possible to delete the gene in experiments to follow without adverse consequences. To confirm the results that had been obtained by the ChIP-on-chip analysis, we performed a ChIP experiment with wild-type cells undergoing sporulation in which *ywjI* DNA was amplified quantitatively by radioactive PCR. The

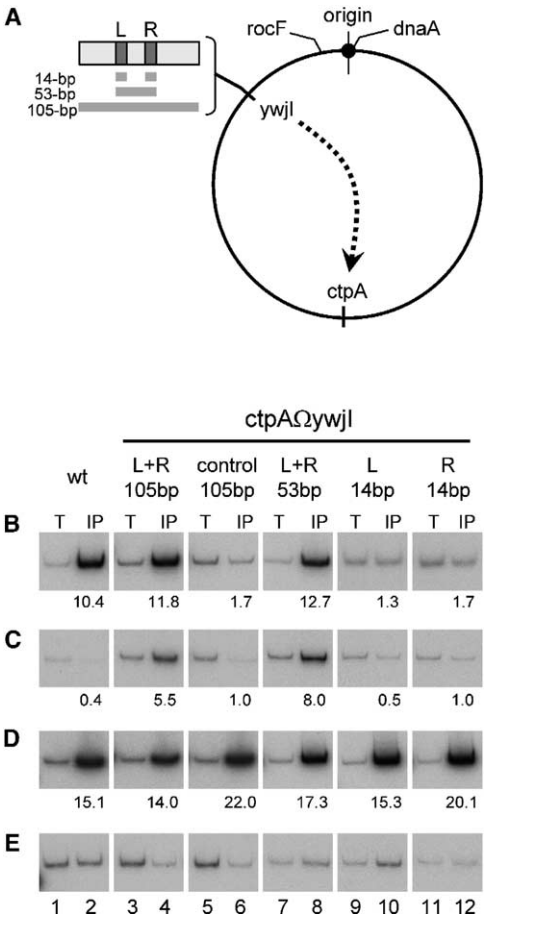

Figure 3. DNA Containing the 14 bp Sequence Motif Is Sufficient to Promote RacA Binding In Vivo

(A) A schematic representation of the relative chromosomal locations of the sites tested by ChIP analysis. Dashed arrow indicates a translocation of a segment of *ywjI* into *ctpA*. The box (upper left) represents the two consensus sequences for RacA binding that are located in *ywjI* region (L, left; R, right). Below, segments (14, 53, and 105 bp) that were used for the translocation experiments (see text for more details).

(B–E) Electropherograms of the products of representative radiolabeled PCR products. PCR amplifications from "total chromosomal DNA" and from DNA precipitated with anti-RacA antibodies (IP) are shown. Samples were prepared from sporulating cells of strains: PY79 (wt; lanes 1 and 2), MF1949 (L + R, 105 bp; lanes 3 and 4), MF1950 (control, 105 bp; lanes 5 and 6), MF2019 (L + R, 53 bp; lanes 7 and 8), MF2017 (L, 14 bp; lanes 9 and 10), and MF2018 (R, 14 bp; lanes 11 and 12). Insertion of the *ywjI* segment into the *ctpA* site is indicated as *ctpAΩywjI*. DNA samples of each strain were PCR amplified from *ywjI* (B), *ctpA* (C), *rocF* (D), and *dnaA* (E) loci. The *dnaA* gene was used as an internal amplification control for normalizing the variations between the different strains. PCR fragments were resolved in a polyacrylamide gel and then band intensities on the autoradiograms were quantitated by using NIH Image software. To account for differences in loading or the variations in amplification with different primer sets, enrichment factors were normalized as: (band intensity of test IP) / (band intensity of *dnaA* IP) and are indicated below each panel. The representative results of three independent experiments are shown.

results showed that immunoprecipitation with anti-RacA antibodies had caused a 10-fold enrichment of *ywjI* (Figure 3B, lanes 1 and 2). As a control and as reported previously (Ben-Yehuda et al., 2003a), little

signal was detected when the ChIP procedure was performed with sporulating cells that were mutant for RacA (data not shown). In contrast, amplification by radiolabeled PCR of *ctpA*, which lacks a potential RacA binding site as judged by bioinformatics analysis, revealed little or no enrichment with RacA antibodies (enrichment factor of 0.4; Figure 3C, lanes 1 and 2), which is in keeping with the findings of the ChIP-on-chip analysis (enrichment factor of 0.6; Table S1). The *ctpA* gene, which is located in the origin-distal region of the chromosome (–2082 kb), is also dispensable both for growth and sporulation and, hence, represented an ideal location for insertion of the putative RacA binding sequences from *ywjI*. As controls, we performed radiolabeled PCR with *rocF* (position –73 kb; representing a positive control; Figure 3D, lanes 1 and 2), which we knew from previous work was enriched by immunoprecipitation with RacA antibodies, and *dnaA* (+0.2 kb; representing a negative control; Figure 3E, lanes 1 and 2), which we knew was not enriched. The enrichment values were in agreement with our previous findings (Ben-Yehuda et al., 2003a), and we used *rocF* and *dnaA* in all of our subsequent experiments as standards for normalizing the results (as explained in the legend to Figure 3).

Next, we deleted *ywjI* and inserted a 105 bp DNA segment from *ywjI* (nucleotide positions 499–603 of its coding sequence) that contained the two adjacent consensus sequences into *ctpA* (Figure 3A). Strikingly, the results show that the presence of the 105 bp insertion was sufficient to increase the enrichment factor for *ctpA* (11.8, Figure 3B, lanes 3 and 4) to a similar level to what had been observed for *ywjI* at its normal position (10.4, Figure 3B, lanes 1 and 2). The presence of the 105 bp insert also caused an increase in the enrichment factor (from 0.4 to 5.5) for sequences flanking the insertion site in *ctpA* (Figure 3C, compare lanes 1 and 2 with lanes 3 and 4). Similar results to those obtained with the 105 bp DNA were obtained when a "minimal" 53 bp segment of *ywjI* (nucleotide positions 525–577) that simply contained the two 14 bp consensus sequences and the 25 bp spacer was inserted into *ctpA* (Figures 3A and 3C, lanes 7 and 8). In contrast, insertion of a 105 bp segment from a region of *ywjI* (nucleotide positions 319–423) that lacked the putative consensus sequences failed to cause a measurable increase in the enrichment factor for *ctpA* (Figures 3B and 3C, lanes 5 and 6). Taken together, these results are consistent with the idea that one or both of the 14 bp consensus sequences in *ywjI* are necessary and sufficient for preferential binding by RacA in vivo.

To investigate whether both consensus sequences are required for binding, we constructed two additional strains in which the *ywjI* consensus sequence on the left (L, nucleotide positions 525–538) and on the right (R, nucleotide positions 564–577 of *ywjI*) were separately inserted at the *ctpA* locus (Figure 3A). Only a small enrichment factor was detected for each of the single consensus-containing constructs (Figures 3B and 3C, lanes 9–12). Thus, neither 14 bp sequence alone was sufficient for tight binding by RacA in vivo.

Purified RacA Interacts with the 14 bp Consensus Sequence

To determine whether RacA recognizes the 14 bp motif directly, we asked whether purified RacA would protect the sequence from the action of DNase I in footprinting experiments. Increasing concentrations of RacA were allowed to bind to ^{32}P-end-labeled DNAs containing at least one putative binding site (Figures 4A–4D). The end-labeled DNAs were treated with DNase I, and the resulting fragments were subjected to electrophoresis. Footprinting was initially performed by using the 105 bp DNA segment from *ywjI*, which contained sufficient sequence information to promote selective binding by RacA in vivo, as demonstrated by the chromosome translocation experiment. The results of Figure 4A demonstrate that RacA protected both the L and the R sites from DNase I digestion and that the regions of protection corresponded closely to the two 14 bp sequences. Next, we asked whether RacA would bind to the L or R sites alone. Figures 3B and 3C (lanes 9–12) showed that neither site alone was sufficient for strong binding by RacA in vivo, but we were able to detect selective binding of RacA to DNAs containing one or the other site in vitro when tested by footprint analysis. Similar results were obtained with *ywhG* (Figure 4D) and *yycJ* (data not shown), which exhibited a high enrichment factor for RacA binding in vivo. Taken together, these results reinforce the view that the 14 bp motif, which we named *ram* for *R*acA binding *m*otif, is the recognition sequence for RacA, and RacA recognizes this sequence directly.

RacA Causes DNA Condensation

RacA binds in a preferential manner to *ram* sites clustered in the origin region of the chromosome and in a nonspecific manner throughout the chromosome (Ben-Yehuda et al., 2003a). We speculated that interactions between RacA molecules bound to *ram* sites could promote the compaction of the centromere-like element into a higher order complex and that interactions between RacA molecules bound nonspecifically throughout the chromosome could be responsible for remodeling the chromosomes into the elongated axial filament (Ben-Yehuda et al., 2003a). To determine whether RacA causes DNA compaction and, if so, whether this compaction involves RacA-RacA interactions, we investigated how RacA acts on non-*ram*-containing DNA in vitro. Our strategy was to measure the effect of RacA on the degree of compaction of individual tethered DNA molecules of phage λ (48.5 kb) as a function of force applied to the DNA. Controlled forces were applied using the "magnetic tweezer" technique in which a magnetic field was used to apply force to a paramagnetic particle attached to the free end of the DNA (Figure 5A) (Skoko et al., 2004). Phage λ (which is not native to *B. subtilis*) lacks specific binding sites for RacA, and hence our experiments involved nonspecific binding of RacA to the DNA.

Figure 5A shows the result of a λ DNA compaction experiment. First, extension of a λ DNA was measured in protein-free buffer as a function of applied force (Figure 5A, open circles); a high force (10 pN) fully extended the DNA to its total 16.5 μm contour length, whereas a low force (0.1 pN) extended the DNA to about half of its total length. Naked DNA displays a reversible force response: at each force there is a certain known extension (Bustamante et al., 2000). After these measure-

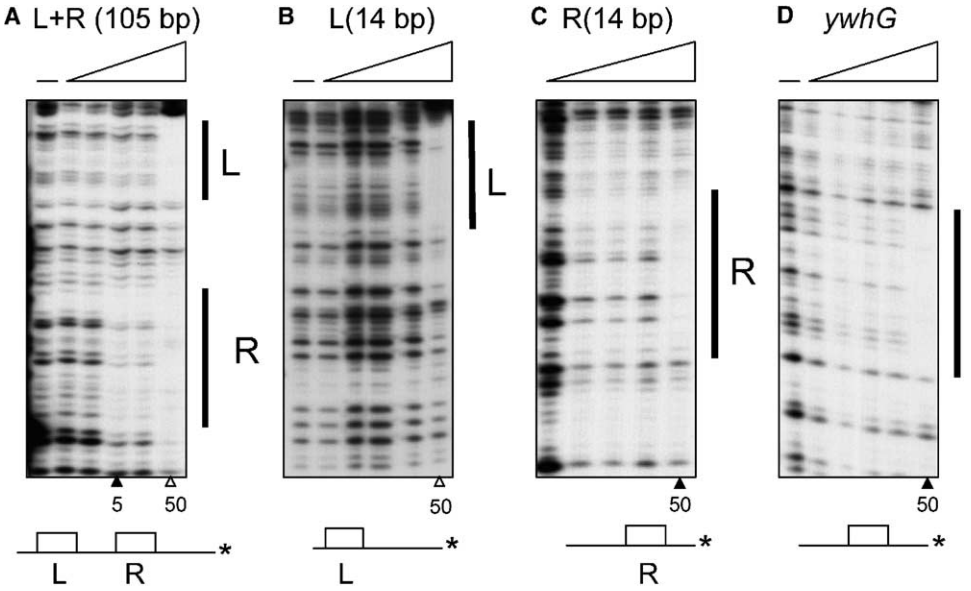

Figure 4. DNase I Footprint Analysis of DNA Regions Containing the Putative 14 bp Sequence Motif for RacA Binding

Each panel represents a set of footprint reactions performed on four end-labeled templates with purified RacA

(A) A 105 bp *ywjI* fragment containing two RacA consensus sites, labeled L (left) and R (right).

(B) A *ywjI* (Left) fragment containing only the 14 bp left consensus site.

(C) A *ywjI* (Right) fragment containing only the 14 bp right consensus site.

(D) A *ywhG* fragment containing a single RacA consensus site. At the bottom of each panel, the asterisk (*) denotes the [γ-^{32}P]ATP end label. The boxes represent the consensus RacA binding sequence, and its position represents its location relative to the end label. The right-angle triangle at the top of each panel represents an increase in RacA protein concentration in the following order: 0.5, 1, 5, 10, and 50 nM, and the dash (–) represents the lane where no RacA was incubated with the labeled template. The unfilled equilateral triangle at the bottom of (A) and (B) represents the lowest concentration where RacA binding is detected to the left consensus site in each template. The filled-in equilateral triangle in (A) and (C) represents the lowest concentration in which RacA binding is detected to the right consensus site of each template. The number below each triangle represents the lowest concentration of RacA (nM) at which binding was detected.

ments, we increased the force to 10 pN, fully extending the molecule. Then, we introduced buffer containing 80 nM of RacA into the sample and made extension measurements at a series of gradually lowered forces (Figure 5A, solid circles, a to b). At the initial high force (10 pN), the length of the DNA was unchanged: RacA was unable to compact the DNA against this force. However, when force was reduced to about 6 pN, we observed that the molecule began to be compacted. As force was reduced further, progressively more compaction occurred. Finally, when force was reduced to 0.6 pN, the length of the molecule had been reduced to about 4.5 μm, about one-third of the full extension for naked DNA in buffer at that force. Thus, RacA by itself is able to condense a single, nonspecific DNA against forces of up to 6 ± 1 pN (error was obtained from three experiments; see Figure S1). The condensation data in Figure 5A were stable extensions obtained at each progressively lower force. The degree of compaction of the RacA-DNA complex relative to bare DNA varied with force; at 0.6 pN the RacA-DNA complex was reduced to only about one-third the length of bare DNA.

Next, we began to increase force in an attempt to open the compacted structure (Figure 5A, solid circles, b to c). Strikingly, even 10 pN forces were unable to restore the DNA to near its full 16.5 μm length, indicating that RacA forms a highly stable, folded complex even with nonspecific DNA. When we allowed RacA to act at low force (~0.1 pN), the DNA was folded into an even more highly condensed structure that required a force of 25 pN to open (data not shown). The condensed structure is likely held together by strong RacA-RacA interactions, as inferred from its extreme stability against force and even exposure to protein-free buffer (data not shown).

We also performed time course experiments in which a RacA-DNA complex was allowed to form at 4.5 pN (Figure 5B) and then was opened by increasing the force to 7 pN (Figure 5C). During folding (Figure 5B), a rather smooth contraction occurred with occasional more rapid runs of compaction of up to 200 nm. When subsequently opened, a pattern of interspersed slow and rapid decompaction was observed (Figure 5C). The overall smooth compaction and decompaction in our experiments at high forces indicate that DNA is being folded tightly into a condensed complex, rather than being loosely looped or crosslinked.

The capacity for RacA to compact λ DNA was highly concentration dependent. In experiments that used 40 nM of RacA, only mild compaction occurred for forces below 1 pN; for 20 nM RacA, no compaction was observed (see Figure S2). We caution that although these concentrations are far below the RacA concentration during sporulation (~3000 molecules per cell, equivalent to ~3 μM), the RacA to DNA ratio in vivo is only about one molecule per 3 kb, whereas in single DNA assay experiments of this type, the protein is in vast excess.

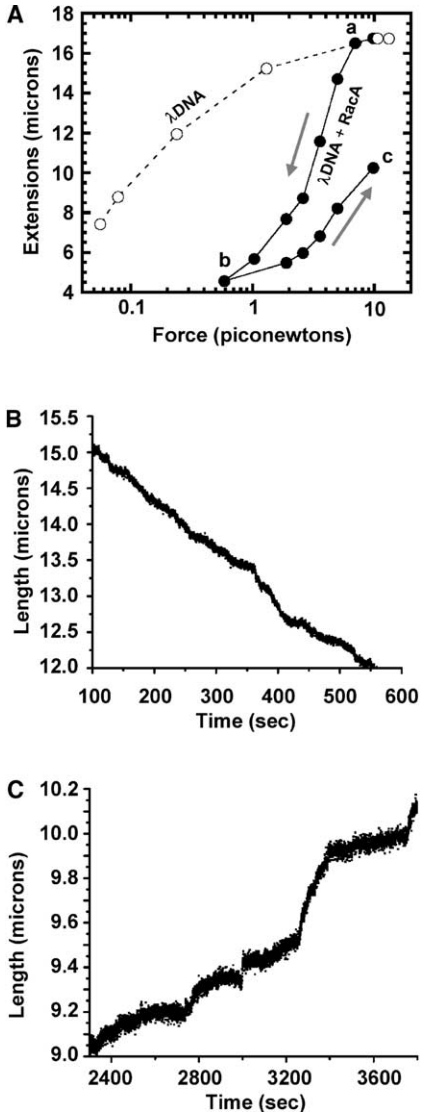

Figure 5. Single DNA Study of RacA Nonsequence-Specific Interactions

(A) DNA end-to-end extension as a function of force. Open circles show measurements for naked DNA in buffer (containing 40 mM NaCl) before addition of RacA protein. Filled circles show DNA extension after RacA is introduced into the flow cell; initially force is at 10 pN (a) and then is gradually reduced (arrows leading to b). Below 6 pN the DNA becomes compacted relative to the naked DNA. When force is increased again (b to c), the DNA remains compacted by RacA.

(B) Extension as a function of time during folding of DNA by RacA against a force of 4.5 pN. The molecule is progressively folded at an overall smooth rate, with occasional jumps down of roughly 100 nm visible.

(C) Extension as a function of time during the subsequent opening of the RacA-DNA complex when using a force of 7 pN. Unfolding takes place more irregularly than folding via a series of jump events distributed over a wide range of lengths from 100–500 nm.

Discussion

The structure of chromosomes in bacteria and eukaryotic cells is dynamic. Chromosomes undergo rapid changes in condensation and architecture during the cell cycle and at various stages of development (Haering and Nasmyth, 2003; Sherratt, 2003). Chromosome segregation upon entry into sporulation in *B. subtilis* involves a specialized system for remodeling and anchoring the chromosomes to the cell poles and therefore provides a unique opportunity to study chromosome organization in a bacterium. Here, we investigated the mechanism by which RacA acts to remodel chromosomes and to anchor them to the cell poles. We identified 25 regions of preferential binding by RacA that define a centromere-like element that extends for 612 kb across the origin-proximal portion of the chromosome, representing 15% of the genome. Interestingly, *racA* is located at the left border of the centromere-like element. Complementary lines of evidence identified a GC-rich, inverted repeat sequence motif of 14 bp, *ram*, as the recognition sequence for RacA. RacA contains a putative helix-turn-helix in its N-terminal region that is required for DNA binding (Ben-Yehuda et al., 2003a), and it seems likely that this domain is responsible for interacting with *ram*. Evidence from experiments in which we monitored the effects of RacA on single DNA molecules revealed that RacA causes DNA to compact dramatically and does so through strong RacA-RacA interactions. The RacA amino acid sequence exhibits two putative coiled-coil structures in its C-terminal region, and it is possible that these domains are responsible for the ability of RacA molecules to interact with each other.

We speculate that RacA molecules bound at the centromere-like element interact with each other to form a single, highly condensed, higher order structure. The formation of this structure could create an adhesive patch that sticks to DivIVA molecules located at the cell pole (Marston et al., 1998; Thomaides et al., 2001). The ability of RacA also to remodel the sister chromosomes of the sporangium into a single elongated filament is most likely mediated by nonspecific RacA-DNA interactions throughout the chromosome. Again, and based on the striking ability of RacA to cause DNA compaction, we propose that the formation of the axial filament is driven in part by the ability of RacA to condense DNA. Differences in the local concentration of RacA between the centromere-like element and the rest of the chromosome may affect the level of DNA compaction. That is, clustering of preferential binding sites for RacA may cause a particularly high degree of compaction in the origin-proximal portion of the chromosome whereas nonspecific interactions of RacA may cause a more modest level of compaction in the remainder of the chromosome.

Wu and Errington (2002) constructed chromosome inversions that led them to identify a portion of the chromosome referred to as the polar localization region (PLR) that is responsible for the polar positioning of the chromosome during sporulation. The PLR is located upstream and to the left of the origin, extending approximately from position –300 kb to position –150 kb (Wu and Errington, 2002). For comparison, the centromere-like element identified here extends from position –412 kb to position +200 kb, straddling (but with a bias to the left of) the origin. Thus, PLR is entirely contained within the centromere-like element. We therefore believe that the PLR represents part of the centromeric region that is recognized by RacA. Perhaps the 150 kb

region defined by the chromosomal inversion analysis represents a minimal portion of the centromere-like element that is required for efficient chromosomal anchoring.

The centromeric element revealed in this study resembles the centromeres of many eukaryotic cells in its large size and diffuse structure. However, eukaryotic centromeres often contain highly repetitive sequences and are highly methylated, inactive heterochromatic regions, which are typically silent for transcription and recombination (Eichler and Sankoff, 2003). In contrast, the *B. subtilis* centromere is unlikely to be silent. It contains early sporulation genes that are activated concurrently with the induction of *racA*, some of which are found at peak regions for RacA binding. Moreover, all of the *ram* sites were located inside protein-coding sequences. We therefore believe that RacA condenses the origin region into a highly compact structure, but it evidently does so without blocking gene expression.

Other than *ram*, few *cis*-acting elements that play a role in chromosome segregation are known in bacteria. Kadoya et al. (2002) reported two elements in the origin region of *B. subtilis* that are involved in chromosome segregation, and Yamaichi and Niki (2004) have described a 25 bp *cis*-acting site in *E. coli* called *migS* that affects bipolar positioning of the origin region. Unlike *ram*, *migS* is present only once in the *E. coli* chromosome, and its function in chromosome segregation is unknown.

Reminiscent of RacA is Spo0J, a *B. subtilis* protein that binds to multiple sites in the origin portion of the chromosome. Spo0J belongs to the ParB family of partitioning proteins, which are involved in both plasmid and chromosome segregation (Gerdes et al., 2004). Spo0J binds to eight 16 bp, inverted repeat sequences (known as *parS*), which are located in the origin-proximal portion of the chromosome where they are distributed over a distance of 800 kb (Lin and Grossman, 1998). Lin and Grossman (1998) proposed that Spo0J causes this 800 kb stretch of DNA to fold into a higher order complex. Mutants of Spo0J have a mild chromosome segregation defect (Sharpe and Errington, 1996), and it is possible that formation of this complex facilitates the separation of newly duplicated origin regions. Nevertheless, no evidence exists to suggest that Spo0J anchors the origin region to a cellular structure involved in chromosome segregation. Hence, it is unlikely that *parS* sites function as a centromere-like element. Wu and Errington (2003) have suggested that Spo0J and its ParA-like partners Soj and RacA have partially redundant functions in capturing the origin region in the forespore compartment, as a triple *soj spo0J racA* mutant exhibited a higher level of chromosome misorientation than the *racA* mutant alone. However, unlike RacA, the absence of Soj-Spo0J is known not to affect chromosome anchoring to the cell poles (Wu and Errington, 2002). We therefore believe that the synthetic phenotype observed in the triple mutant is an indirect consequence of the effects of the absence of Soj-Spo0J on cell length and chromosome copy number (Webb et al., 1997; Lee et al., 2003) rather than a direct effect on capturing the origin region.

The capacity of RacA to compact DNA can be compared to that of condensins, which are bacterial and eukaryotic protein complexes that cause chromosome condensation. Condensins typically consist of two SMC (structural maintenance of chromosomes) subunits and two or three non-SMC proteins (Hirano, 2002; Haering and Nasmyth, 2003). SMC polypeptide chains fold back on themselves to form an ATP binding globular domain that has a tail consisting of an extended, antiparallel coiled coil. Deletion of the *smc* gene or its counterparts in bacteria causes temperature-sensitive growth, nucleoid decondensation, and chromosomal partitioning defects (Niki et al., 1991; Britton et al., 1998; Moriya et al., 1998; Jensen and Shapiro, 1999). Interestingly, RacA resembles SMC in having a putative coil-coiled domain (with the potential of forming two such structures), but RacA contains a putative helix-turn-helix at its N terminus in place of the ATP binding, globular domain of SMC proteins. Thus RacA-mediated DNA condensation does not consume energy. Instead, it relies on strong protein-protein interactions to bring about DNA compaction. The high stability of the RacA-DNA complex is quite distinct among bacterial proteins that have been studied micromechanically: the complexes formed by the DNA-bending proteins IHF (Ali et al., 2001) and HU (van Noort et al., 2004; Skoko et al., 2004) can be extended to nearly the full original DNA contour length by force in a few seconds, unlike RacA-DNA complexes.

In summary, RacA resembles the ParB family member Spo0J in that it binds to multiple sites clustered in the origin region of the chromosome, and it resembles SMC in its structure and in its capacity to cause DNA compaction. Unlike Spo0J and SMC, however, RacA functions as a kinetichore in that it interacts with a large, defined, centromeric-like DNA element to anchor the chromosome to a conspicuous cellular structure and thereby ensures proper chromosome segregation.

Experimental Procedures

Strains and Plasmids

B. subtilis strains were derivatives of PY79 (Youngman et al., 1984) and are listed in Table S3. Plasmid constructions are described in the Supplemental Data.

General Methods

Sporulation was induced by transferring cells growing in hydrolyzed casein (CH) medium to the resuspension medium of Sterlini and Mandelstam (1969; Harwood and Cutting, 1990). Growth and sporulation were carried out at 30°C. Time of sporulation was measured from the time of suspension in sporulation medium. Competent cells were prepared as described previously (Dubnau and Davidoff-Abelson, 1971; Sambrook et al., 1989).

ChIP and ChIP-on-Chip Experiments

ChIP experiments and quantitative radioactive PCR analyses were performed as described previously (Ben-Yehuda et al., 2003a). Differential fluorescent labeling, hybridization to microarrays, and array scanning (ChIP-on-chip) were done as described elsewhere (Britton et al., 2002; Molle et al., 2003). The arrays used for this study were spotted with 4074 PCR products corresponding to *B. subtilis* ORFs as well as with four *E. coli* genes as negative controls (Britton et al., 2002). The hybridization results were scanned by using a GenePix 4000B scanner (Axon Instruments) and analyzed with Genepix 3.0 software (Axon Instruments). For details on the bioinformatics analyses of RacA ChIP-on-chip data see the Supplemental Data.

DNase I Footprinting

All DNA fragments used for footprinting were generated by PCR amplification in which one of the two paired oligonucleotide primers (100 pmol) was end labeled with 80 μCi of [γ-^{32}P]ATP (NEG002A, New England Nuclear) by T4 Polynucleotide Kinase (New England Biolabs) (for details see the Supplemental Data). The PCR product was run out on a 1% agarose gel and gel purified (QIAquick Gel Extraction Kit, Qiagen Inc.). A portion of the gel-purified product was subjected to scintillation counting, and a normalized volume of end-labeled DNA (to 30,000 cpm) was used per footprinting reaction. Purified RacA-his6 (see the Supplemental Data) was added to the end-labeled DNA at the described concentrations in Footprinting Buffer (20 mM Tris-HCl [pH 8.0], 5 mM $MgCl_2$, 5 mM $CaCl_2$, 0.1 mM DTT, 0.1 mM EDTA, 50 μg/ml BSA) and allowed to bind at RT for 10 min. 2 μl of DNaseI (1:50 dilution of 1 U/μl; Invitrogen Life Sciences) was added to the reaction mixture for 30 s, and the reaction was stopped by the addition of 25 μl STOP solution (1.5 M sodium acetate [pH 5.3], 20 mM EDTA, 400 μg/ml glycogen). The DNA was precipitated in ice-cold ethanol, washed in 70% Ethanol, and resuspended in Formamide DNA loading buffer. The resuspended DNA was boiled, run on an 8% sequencing gel (SequaGel Sequencing System, National Diagnostics Inc.), and exposed to phosphorimaging (VersaDoc) and/or autoradiography. Primer pairs used for this study are listed in Table S3.

Single DNA Protein Binding Assay

Labeled λ DNA molecules (Promega, Madison, WI) were prepared by ligation of biotin- and digoxygenin-labeled oligomers (Proligo, San Diego, CA) onto the cos ends (Smith et al., 1992; Skoko et al., 2004). Cover glasses were prepared for DNA binding first by oxygen plasma cleaning, binding of aminosilane (Sigma), then glutaraldehyde (Sigma), and finally antidigoxigenin (Roche) as previously described (Skoko et al. 2004). This prepared glass was used as one surface of a flow cell for experiments.

Labeled DNAs were incubated with streptavidin-labeled, 2.8 μm paramagnetic particles (Dynal), injected into the flow cell, and allowed to settle onto the antidig-labeled surface. After a 5 min incubation, the flow cell was inverted and placed onto a custom-built microscope, which was set up to allow observation of the beads near the treated surface and to position permanent magnets so as to adjust forces applied to the beads. Details of this setup and force calibration procedures are discussed in Skoko et al. (2004) and follow the methods of Strick et al. (1998). All experiments used buffer containing 20 mM HEPES and 40 mM NaCl, adjusted to pH 7.5.

Supplemental Data

Supplemental Data including two figures, four tables, and Supplemental Experimental Procedures are available online with this article at http://www.molecule.org/cgi/content/full/17/6/773/DC1/.

Acknowledgments

S.B.-Y. was a Human Frontier Science Program (HFSP) postdoctoral scholar at the laboratory of R.L. and is currently supported by the Career Development Award (CDA) of the HFSP and the Israel Science Foundation (ISF grant 1401/04). The work at the laboratory of R.L. (Harvard) was supported by National Institutes of Health grant GM18568. The work at the laboratory of J.F.M. (University of Illinois at Chicago) was supported in part by National Science Foundation grants DMR-0203963 and MCB-0240998 and by a Focused Giving grant from Johnson and Johnson Corporation. J.S.L. (Harvard) was supported by NSF grant DMS-0244638.

Received: October 5, 2004
Revised: January 16, 2005
Accepted: February 16, 2005
Published: March 17, 2005

References

Ali, B.M., Amit, R., Braslavsky, I., Oppenheim, A.B., Gileadi, O., and Stavans, J. (2001). Compaction of single DNA molecules induced by binding of integration host factor (IHF). Proc. Natl. Acad. Sci. USA *98*, 10658–10663.

Ausmees, N., and Jacobs-Wagner, C. (2003). Spatial and temporal control of differentiation and cell cycle progression in Caulobacter crescentus. Annu. Rev. Microbiol. *57*, 225–247.

Ben-Yehuda, S., Rudner, D.Z., and Losick, R. (2003a). RacA, a bacterial protein that anchors chromosomes to the cell poles. Science *299*, 532–536. Published online December 19, 2002. 10.1126/science.1079914.

Ben-Yehuda, S., Rudner, D.Z., and Losick, R. (2003b). Assembly of the SpoIIIE DNA translocase depends on chromosome trapping in Bacillus subtilis. Curr. Biol. *13*, 2196–2200.

Britton, R.A., Lin, D.C., and Grossman, A.D. (1998). Characterization of a prokaryotic SMC protein involved in chromosome partitioning. Genes Dev. *12*, 1254–1259.

Britton, R.A., Eichenberger, P., Gonzalez-Pastor, J.E., Fawcett, P., Monson, R., Losick, R., and Grossman, A.D. (2002). Genome-wide analysis of the stationary-phase sigma factor (sigma-H) regulon of Bacillus subtilis. J. Bacteriol. *184*, 4881–4890.

Bustamante, C., Smith, S.B., Liphardt, J., and Smith, D. (2000). Single-molecule studies of DNA mechanics. Curr. Opin. Struct. Biol. *10*, 279–285.

Conlon, E.M., Liu, X.S., Lieb, J.D., and Liu, J.S. (2003). Integrating regulatory motif discovery and genome-wide expression analysis. Proc. Natl. Acad. Sci. USA *100*, 3339–3344.

Dubnau, D., and Davidoff-Abelson, R. (1971). Fate of transforming DNA following uptake by competent Bacillus subtilis. I. Formation and properties of the donor-recipient complex. J. Mol. Biol. *56*, 209–221.

Eichler, E.E., and Sankoff, D. (2003). Structural dynamics of eukaryotic chromosome evolution. Science *301*, 793–797.

Gerdes, K., Moller-Jensen, J., Ebersbach, G., Kruse, T., and Nordstrom, K. (2004). Bacterial mitotic machineries. Cell *116*, 359–366.

Glaser, P., Sharpe, M.E., Raether, B., Perego, M., Ohlsen, K., and Errington, J. (1997). Dynamic, mitotic-like behavior of a bacterial protein required for accurate chromosome partitioning. Genes Dev. *11*, 1160–1168.

Gonczy, P., and Hyman, A.A. (1996). Cortical domains and the mechanisms of asymmetric cell division. Trends Cell Biol. *6*, 382–387.

Haering, C.H., and Nasmyth, K. (2003). Building and breaking bridges between sister chromatids. Bioessays *25*, 1178–1191.

Harwood, C.R., and Cutting, S.M. (1990). Molecular Biological Methods for Bacillus (New York: John Wiley and Sons).

Hirano, T. (2002). The ABCs of SMC proteins: two-armed ATPases for chromosome condensation, cohesion, and repair. Genes Dev. *16*, 399–414.

Horvitz, H.R., and Herskowitz, I. (1992). Mechanisms of asymmetric cell division: two Bs or not two Bs, that is the question. Cell *68*, 237–255.

Iyer, V.R., Horak, C.E., Scafe, C.S., Botstein, D., Snyder, M., and Brown, P.O. (2001). Genomic binding sites of the yeast cell-cycle transcription factors SBF and MBF. Nature *409*, 533–538.

Jensen, R.B., and Shapiro, L. (1999). The *Caulobacter crescentus smc* gene is required for cell cycle progression and chromosome segregation. Proc. Natl. Acad. Sci. USA *96*, 10661–10666.

Jensen, R.B., Wang, S.C., and Shapiro, L. (2002). Dynamic localization of proteins and DNA during a bacterial cell cycle. Nat. Rev. Mol. Cell Biol. *3*, 167–176.

Kadoya, R., Hassan, A.K., Kasahara, Y., Ogasawara, N., and Moriya, S. (2002). Two separate DNA sequences within oriC participate in accurate chromosome segregation in Bacillus subtilis. Mol. Microbiol. *45*, 73–87.

Laub, M.T., Chen, S.L., Shapiro, L., and McAdams, H.H. (2002). Genes directly controlled by CtrA, a master regulator of the Caulobacter cell cycle. Proc. Natl. Acad. Sci. USA *99*, 4632–4637.

Lee, P.S., Lin, D.C., Moriya, S., and Grossman, A.D. (2003). Effects of the chromosome partitioning protein Spo0J (ParB) on oriC posi-

tioning and replication initiation in Bacillus subtilis. J. Bacteriol. *185*, 1326–1337.

Lin, D.C., and Grossman, A.D. (1998). Identification and characterization of a bacterial chromosome partitioning site. Cell *92*, 675–685.

Lin, D.C., Levin, P.A., and Grossman, A.D. (1997). Bipolar localization of a chromosome partition protein in Bacillus subtilis. Proc. Natl. Acad. Sci. USA *94*, 4721–4726.

Liu, X.S., Brutlag, D.L., and Liu, J.S. (2002). An algorithm for finding protein-DNA binding sites with applications to chromatin-immunoprecipitation microarray experiments. Nat. Biotechnol. *20*, 835–839.

Madden, K., and Snyder, M. (1998). Cell polarity and morphogenesis in budding yeast. Annu. Rev. Microbiol. *52*, 687–744.

Marston, A.L., Thomaides, H.B., Edwards, D.H., Sharpe, M.E., and Errington, J. (1998). Polar localization of the MinD protein of Bacillus subtilis and its role in selection of the mid-cell division site. Genes Dev. *12*, 3419–3430.

Molle, V., Fujita, M., Jensen, S.T., Eichenberger, P., Gonzalez-Pastor, J.E., Liu, J.S., and Losick, R. (2003). The Spo0A regulon of Bacillus subtilis. Mol. Microbiol. *50*, 1683–1701.

Moriya, S., Tsujikawa, E., Hassan, A.K., Asai, K., Kodama, T., and Ogasawara, N. (1998). A *Bacillus subtilis* gene-encoding protein homologous to eukaryotic SMC motor protein is necessary for chromosome partition. Mol. Microbiol. *29*, 179–187.

Nelson, W.J. (2003). Adaptation of core mechanisms to generate cell polarity. Nature *422*, 766–774.

Niki, H., Jaffe, A., Imamura, R., Ogura, T., and Hiraga, S. (1991). The new gene *mukB* codes for a 177 kd protein with coiled-coil domains involved in chromosome partitioning of *E. coli*. EMBO J. *10*, 183–193.

Piggot, P.J., and Losick, R. (2001). Sporulation genes and intercompartmental regulation. In Bacillus subtilis and Its Closest Relatives: From Genes to Cells, A.L. Sonenshein, J. Hoch, and R. Losick, eds. (Washington, D.C.: ASM Press), pp. 483–517.

Ren, B., Robert, F., Wyrick, J.J., Aparicio, O., Jennings, E.G., Simon, I., Zeitlinger, J., Schreiber, J., Hannett, N., Kanin, E., et al. (2000). Genome-wide location and function of DNA binding proteins. Science *290*, 2306–2309.

Ryter, A., Schaeffer, P., and Ionesco, H. (1966). Classification cytologique, par leur stade de blocage, des mutants de sporulation de Bacillus subtilis Marburg. Ann. Inst. Pasteur (Paris) *110*, 305–315.

Sambrook, J., Fritsch, E.F., and Maniatis, T. (1989). Molecular Cloning: A Laboratory Manual (Cold Spring Harbor, NY: Cold Spring Harbor Laboratory Press).

Scheres, B., and Benfey, P.N. (1999). Asymmetric Cell Division In Plants. Annu. Rev. Plant Physiol. Plant Mol. Biol. *50*, 505–537.

Sharpe, M.E., and Errington, J. (1996). The Bacillus subtilis soj-spo0J locus is required for a centromere-like function involved in prespore chromosome partitioning. Mol. Microbiol. *21*, 501–509.

Sherratt, D.J. (2003). Bacterial chromosome dynamics. Science *301*, 780–785.

Skoko, D., Wong, B., Johnson, R.C., and Marko, J.F. (2004). Micromechanical analysis of the binding of DNA-bending proteins HMGB1, NHP6A and HU reveals their ability to form highly stable DNA-protein complexes. Biochemistry *43*, 13867–13874.

Smith, S.B., Finzi, L., and Bustamante, C. (1992). Direct mechanical measurements of the elasticity of single DNA molecules by using magnetic beads. Science *258*, 1122–1126.

Sterlini, J.M., and Mandelstam, J. (1969). Commitment to sporulation in Bacillus subtilis and its relationship to development of actinomycin resistance. Biochem. J. *113*, 29–37.

Stragier, P., and Losick, R. (1996). Molecular genetics of sporulation in Bacillus subtilis. Annu. Rev. Genet. *30*, 297–341.

Strick, T.R., Allemand, J.F., Bensimon, D., and Croquette, V. (1998). Behavior of supercoiled DNA. Biophys. J. *74*, 2016–2028.

Thomaides, H.B., Freeman, M., El Karoui, M., and Errington, J. (2001). Division site selection protein DivIVA of Bacillus subtilis has a second distinct function in chromosome segregation during sporulation. Genes Dev. *15*, 1662–1673.

van Noort, J., Verbrugge, S., Goosen, N., Dekker, C., and Dame, R.T. (2004). Dual architectural roles of HU: formation of flexible hinges and rigid filaments. Proc. Natl. Acad. Sci. USA *101*, 6969–6974.

Webb, C.D., Teleman, A., Gordon, S., Straight, A., Belmont, A., Lin, D.C., Grossman, A.D., Wright, A., and Losick, R. (1997). Bipolar localization of the replication origin regions of chromosomes in vegetative and sporulating cells of B. subtilis. Cell *88*, 667–674.

Wu, L.J., and Errington, J. (1994). Bacillus subtilis spoIIIE protein required for DNA segregation during asymmetric cell division. Science *264*, 572–575.

Wu, L.J., and Errington, J. (1997). Septal localization of the SpoIIIE chromosome partitioning protein in Bacillus subtilis. EMBO J. *16*, 2161–2169.

Wu, L.J., and Errington, J. (2002). A large dispersed chromosomal region required for chromosome segregation in sporulating cells of Bacillus subtilis. EMBO J. *21*, 4001–4011.

Wu, L.J., and Errington, J. (2003). RacA and the Soj-Spo0J system combine to effect polar chromosome segregation in sporulating Bacillus subtilis. Mol. Microbiol. *49*, 1463–1475.

Yamaichi, Y., and Niki, H. (2004). migS, a cis-acting site that affects bipolar positioning of oriC on the Escherichia coli chromosome. EMBO J. *23*, 221–233.

Youngman, P., Perkins, J.B., and Losick, R. (1984). Construction of a cloning site near one end of Tn917 into which foreign DNA may be inserted without affecting transposition in Bacillus subtilis or expression of the transposon-borne erm gene. Plasmid *12*, 1–9.